Radio and optical properties of faint radio population

Loretta Gregorini[1,2], *Isabella Prandoni*[1], *Paola Parma*[1], *Mark H. Wieringa*[3], *Hans R. de Ruiter*[1,4], *Arturo Mignano*[1], *Giampaolo Vettolani*[1], *Ron D. Ekers*[3]

1 INAF-Istituto di Radioastronomia Bologna Italy

2 Dipartimento di Fisica Universita' di Bologna Italy

3 CSIRO Australia Telescope National Facility Epping Australia

4 INAF- Osservatorio Astronomico di Bologna Italy

Summary

We used the ATCA to follow-up at 5 GHz the region previously covered by the sub-mJy ATESP 1.4 GHz survey (*Prandoni et al. 2000a, b*).

We imaged a 1 square degree area where, in addition to the 1.4 GHz information, extensive UBVRIJK$_s$ deep optical imaging is available through the multicolor ESO Deep Public Survey (DPS, *Mignano et al. 2006*, *Olsen et al. 2006*).

The 1.4 and 5 GHz information allowed us to study the radio spectral properties of the ATESP radio sources. We found a significant flattening of the 1.4-5 GHz spectral indeces going to fainter fluxes: the fraction of sources with flat/inverted spectra increases from 38% at S > 4 mJy up to 63% at S < 4 mJy.

We then used the optical information available to assess the nature of the ATESP sub-mJy sources and the physical processes responsible for such a flattening. Preliminary results indicate that flat/inverted sources are more probably triggered by nuclear activity than by star formation.

The faint radio population is a mixture of different classes of objects:

- **Low-luminosity/high-z AGNs, dominating at sub-mJy and mJy fluxes**
- **Normal elliptical galaxies, dominating at sub-mJy and mJy fluxes**
- **Spiral galaxies**
- **Star-forming galaxies, dominating at micro-Jy fluxes**

The relative fractions and the cosmological evolution of the different classes of objects are still quite uncertain.

Multi-frequency radio data with high resolution may help to constrain the origin of the radio emission in the faint radio sources (AGN/star-formation) and may actually be fundamental for understanding eventual links to the optical light.

The ATESP SURVEY: Radio Data

The ATESP survey was carried out with the Australia Telescope Compact Array

1.4 GHz ATESP Survey:

- **26 square degrees at $\delta = -40$**
- **~ 8 arcsec resolution**
- **2967 sources catalogued down to ~ 0.5 mJy**

(*Prandoni et al. 2000a, b)*

5 GHz ATESP Survey:

- **1 square degree at $\delta = -40$**
- **~ 2 arcsec resolution**
- **111 sources catalogued down to ~ 0.4 mJy**

(*Prandoni et al. 2006*)

ATESP source counts at 5 GHz

Using the 111 sources detected at 5 GHz, we improve significantly the statistics in the flux range 0.4 – 1 mJy at 5 GHz.

No evidence of flattening or slope change down to the survey limit.

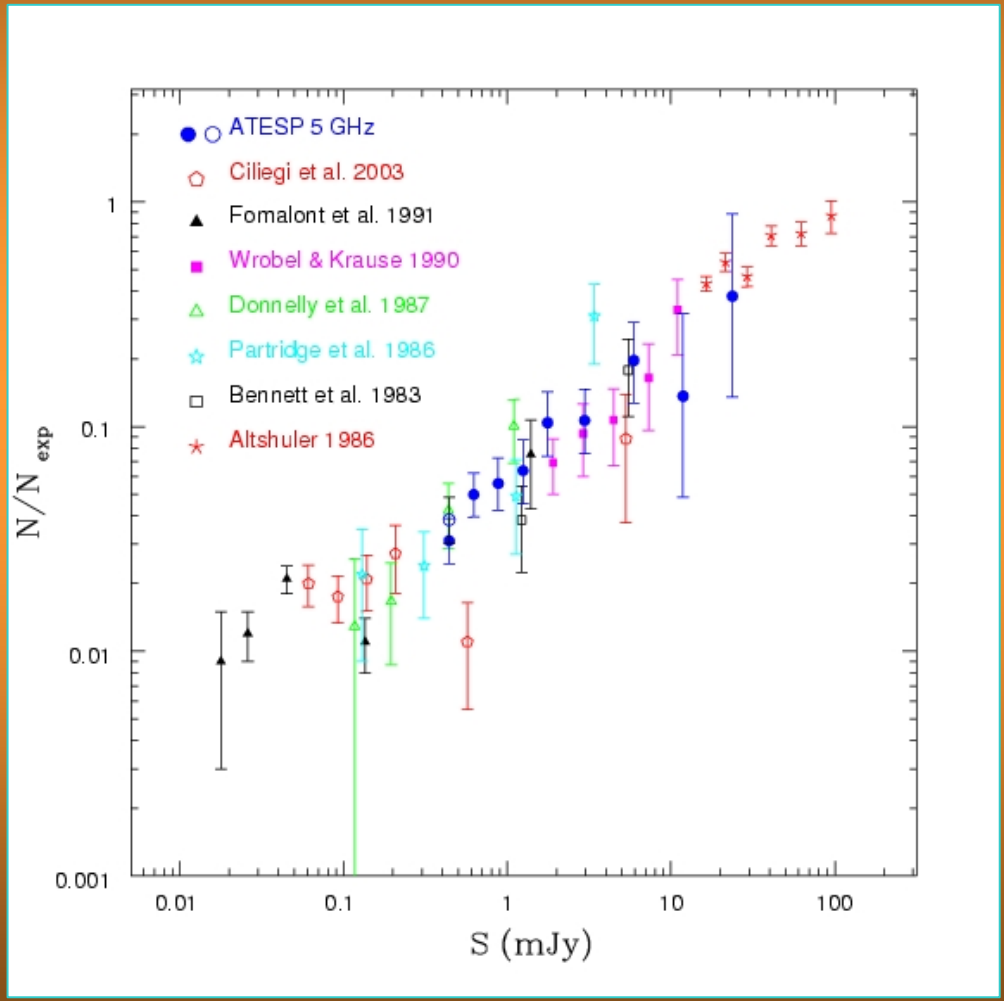

Source counts normalized to a non evolving Euclidean model

Radio Spectra analysis

- The measured spectral index α (where $S = \nu^{\alpha}$) between 1.4 and 5 GHz shows a significant flattening with decreasing flux.
- At mJy level radiosources are characterised by steep spectrum ($\alpha \sim 0.7$), as expected for standard synchrotron radio emission.
- At sub-mJy flux densities the sample selected at 5 GHz shows that ~60% of the sources have flat spectra ($\alpha > -0.5$) and a significant fraction (~30%) inverted spectra ($\alpha > 0$).

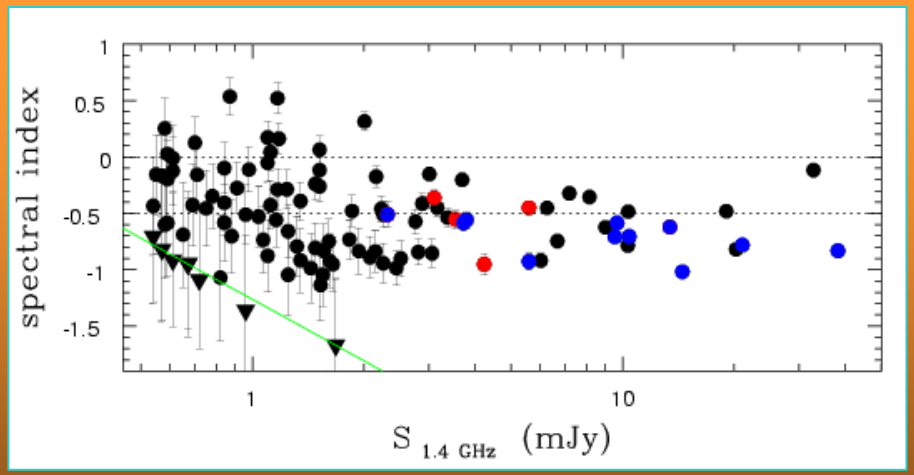

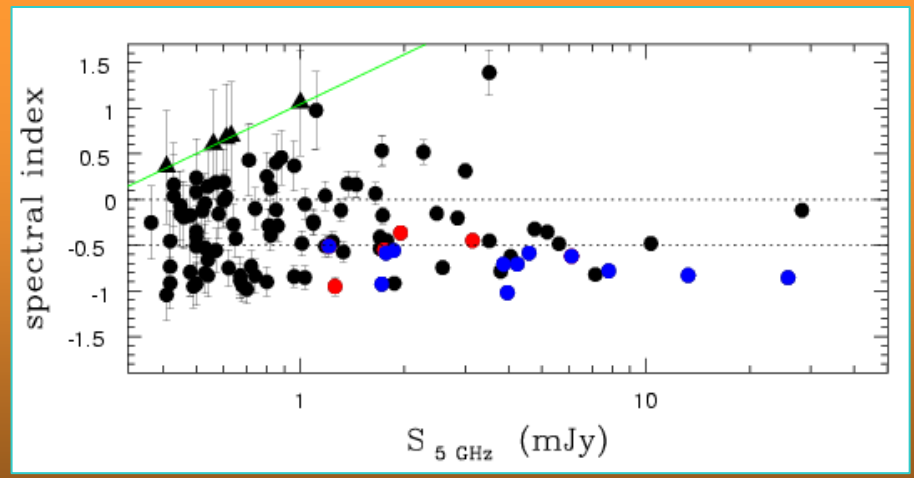

Radiosources with a multiple-component/extended radio morphology, typical of classical AGN driven radio galaxies, are shown in blue and red colours. The green line indicates the 3 sigma detection limit.

Radio Spectra analysis

The radio spectral index statistics for the sample selected at 1.4 and at 5 GHz.

Table 1: Spectral index statistics

Flux range	N	α_{mean}	α_{med}	$N_{\alpha>-0.5}$	$N_{\alpha>0}$
1.4 GHz					
Any flux	109	-0.56 ± 0.04	−0.57	47 (43%)	10 (9%)
$S > 4$ mJy	22	-0.66 ± 0.06	−0.71	7 (32%)	-
$S \leq 4$ mJy	87	-0.53 ± 0.05	−0.53	40 (46%)	10 (11%)
5 GHz					
Any flux	111	-0.28 ± 0.05	−0.40	67 (60%)	28 (25%)
$S > 4$ mJy	13	-0.58 ± 0.06	−0.62	5 (38%)	-
$S \leq 4$ mJy	98	-0.24 ± 0.05	−0.29	62 (63%)	28 (29%)

A general agreement is found with *Fomalont et al. (1991)* who report a $\alpha_{med} = -0.38$ and a $f(\alpha > -0.5) = 60\%$ at fluxes $16 < S_{5\,GHz} < 1000$ μJy; while *Donnelly et al. (1987)* report $\alpha_{mean} = -0.31 \pm 0.58$, $\alpha_{med} = -0.42$ and $f(\alpha > -0.5) = 50\%$ at $0.4 < S_{5\,GHz} < 1.2$ mJy).

On the other hand, a somewhat steeper behaviour was found by *Donnelly et al. (1987)* at 1.4 GHz: $\alpha_{mean} = 0.80 \pm 0.49$, $\alpha_{med} = -0.76$ and $f(\alpha > -0.5) = 22\%$ at $0.5 < S_{1.4\,GHz} < 3$ mJy, which was interpreted as due to a significantly different composition on the faint radio population depending of the selection frequency.

The ATESP SURVEY: Optical Data

- **The ATESP 5 GHz region was imaged in several optical and infrared passbands in the framework of the ESO *Deep Public Survey* (DPS), which comprises three 1 square degree regions (DEEP1, 2, 3) in the southern sky.**
- **The DPS was carried out in the optical (U, B, V, R, I), using the WFI (Wide Field Imager) camera mounted at the 2.2mt ESO telescope, and in the near infrared (J, K_s), using the SOFI camera mounted at the ESO NTT telescope.**
- **The DEEP1 (the DPS region which overlaps with the ATESP) has typical depths of $U_{AB} \sim 25.7$, $B_{AB} \sim 25.5$, $V_{AB} \sim 25.2$, $R_{AB} \sim 24.8$, $I_{AB} \sim 24.1$ (*Mignano et al. 2006*).**
- **The observations in K_s-band ($K_{s\,AB} \leq 21.3$), were obtained for about half the area covered by the optical survey. For a more limited region, deep ($J_{AB} \leq 23.4$ and $K_{s\,AB} \leq 22.7$) infrared images are available (*Olsen et al. 2006*)**

Identification in the ATESP-DEEP1

We performed a cross-correlation between the DPS optical and the ATESP radio catalogues using the "*Likelihood Ratio technique*". It was possible to identify 74% (63/85) of the ATESP-DEEP1 radiosources, with an estimated contamination rate of 7%. The identification statistics is in a good agreement with what found in the literature for other deep radio samples, identified down to similar optical/near infrared depths (e.g. the VVDS-VLA and the Phoenix Deep Survey).

Survey	S_{lim} (mJy)	(N_{rad})	area (sq.degr.)	I_{lim}	$\%_{id}$
VVDS–VLA	0.08	1054	1	25	74.0
Phoenix	0.1	839	3	25	79.0
VLA–LH	0.05	63	0.03	24.5	92.0
ATESP–EIS	0.4	386	3	22.5	57.3
ATESP–DEEP1	**0.4**	**85**	**0.5**	**25**	**74.1**

Photometry Checks

We exploited the extensive U, B, V, R, I, J, K_s information to get photometric redshifts and spectral types for the identified radiosources.

To get good z_{phot} is mandatory to have good photometric calibration!

Traditional techniques (e.g. number counts) are not very sensitive to small color systematic offsets (*Mignano et al. 2006*).

We therefore performed a comparison between the colours of DPS stars and colours of the stars as modeled by *Girardi et al. (2005)*. This analysis allowed us to correct U magnitudes: U→ U–0.15.

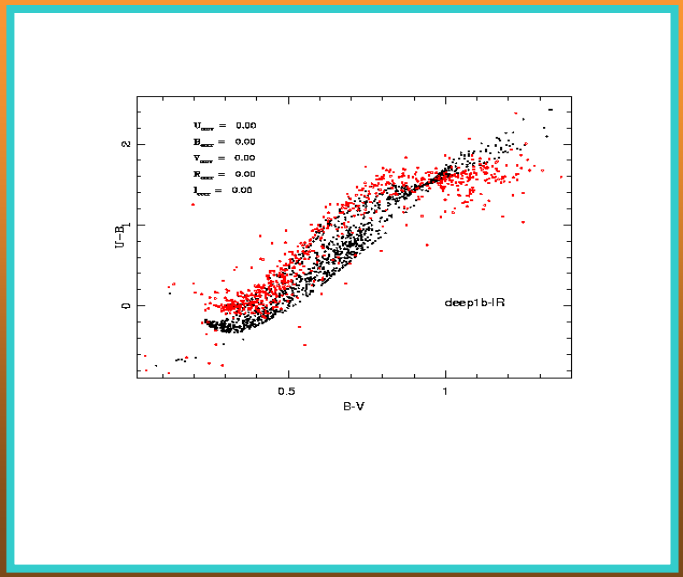

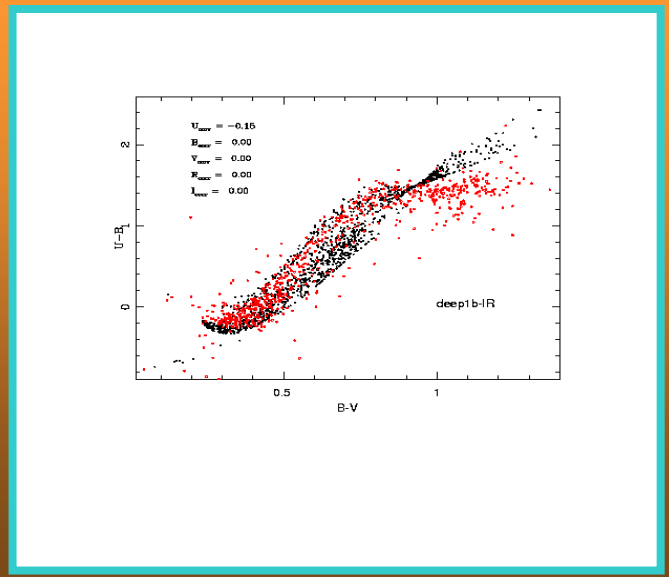

Photometric Spectra

We used Hyperz (Bolzonella et al. 2000) to determine spectral types and photometric redshifts of the 42 ATESP radiosources identified in the 0.5 square degree area of DEEP1, where extensive colour information is available.

We used the default (empirical and synthetic) SEDs provided by Hyperz to describe the different galaxy populations (from normal galaxies to quasars). In addition we have considered some peculiar quasar SEDs, directly downloaded from the SDSS web pages.

Examples are shown in the figures.

StarBurst

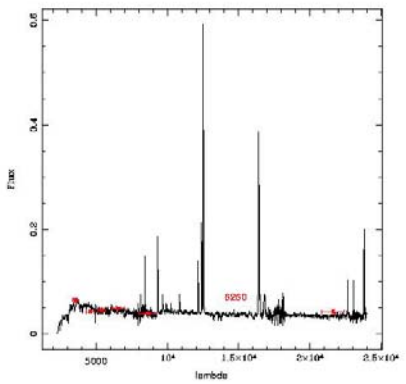

Quasar

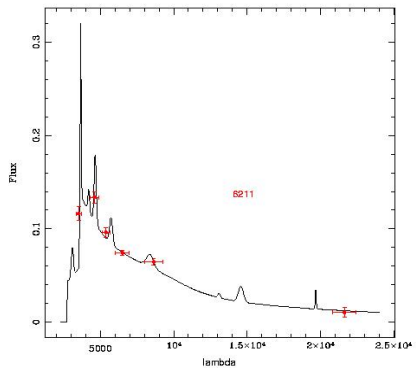

Elliptical

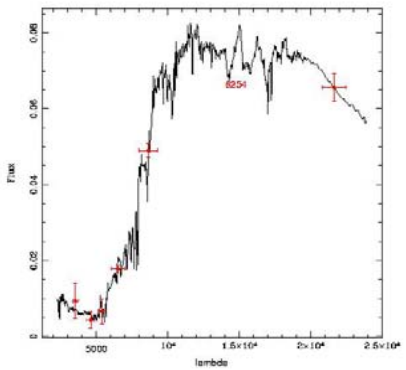

Radio and Optical Properties

In addition to the ATESP data described above, we used optical imaging from the shallower EIS-WIDE survey (I < 22.5, *Nonino et al. 1999*) and related spectroscopy (*Prandoni et al. 2001b*).

From the analysis we have found:

a) most of the flat-spectrum radio sources have high radio-to-optical ratios (R > 1000), typically associated to classical powerful radio galaxies and quasars;

b) flat-spectrum sources with low R values are preferentially identified with early-type galaxies, where the radio emission is probably triggered by low-luminosity AGNs. This is probably the most interesting result, as it could provide new hints on the accreting mechanism of the central black hole;

c) star-forming galaxies are instead typically associated to steep-spectrum sources, as expected for synchrotron emission in galactic disks or in nuclear starbursts.

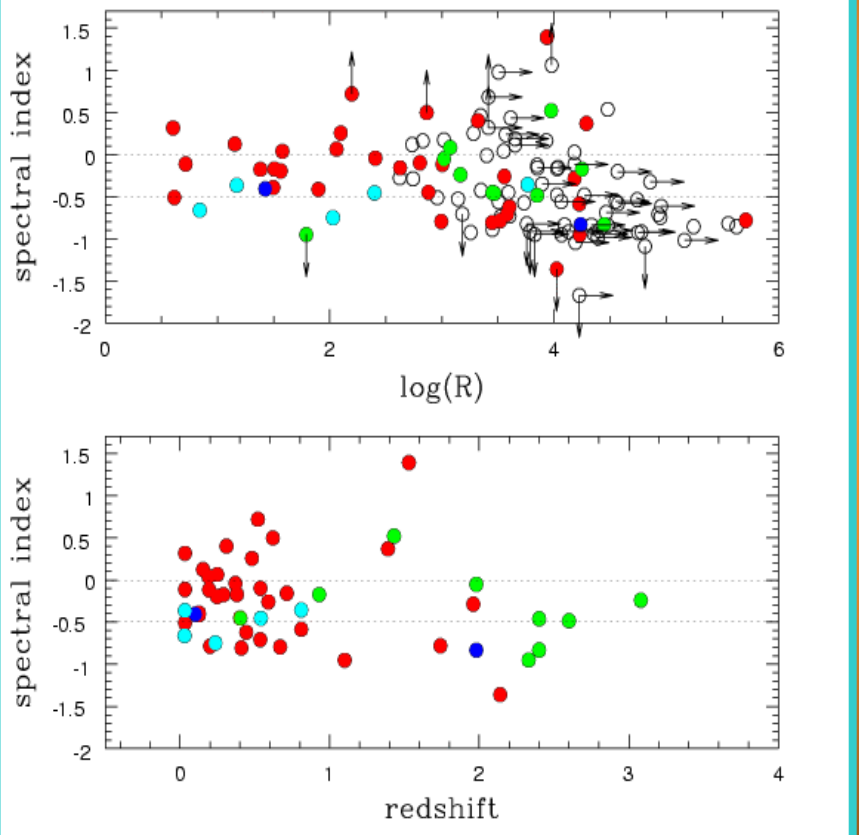

- **AGN**
- **LTS** (Late Type Galaxy)
- **ETS** (Early Type Galaxy)
- **SB** (Star- burst Galaxy)

Sample Redshift distribution

Redshift Distribution:

Early type galaxies **(ETS) extend up to z = 2, showing a significant peak at z = 0.7, while *quasars* (QSO) have higher redshifts (up to z = 5).**

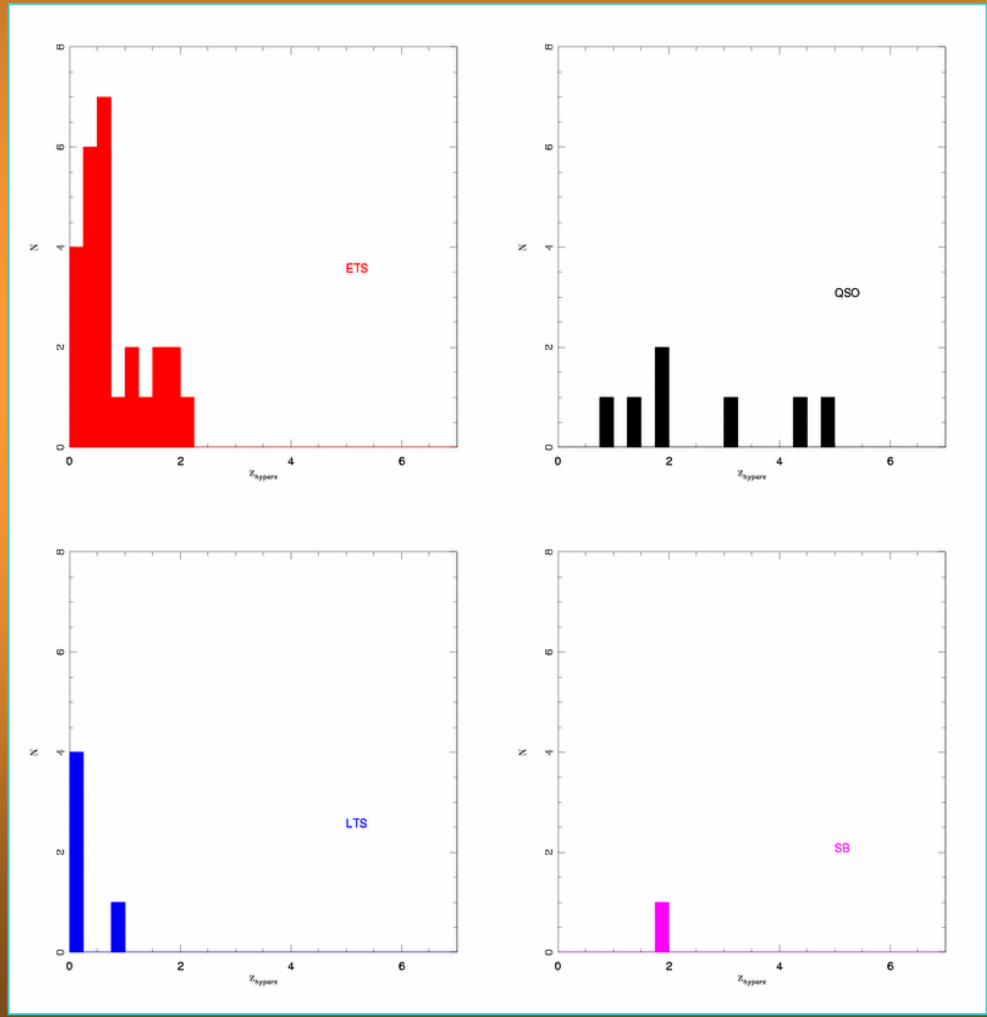

Sample Properties

Composition - out of 42 identified ATESP radiosources:

57% are early type galaxies (Elliptical, S0 and Sa galaxies);

14% are quasars;

14% are late type galaxies (Sb, Sc and starburst galaxies;

15% are objects could not be classified.

Radio Power Distribution: ETS have typically radio luminosities of the order of $10^{23\text{-}25}$ WHz^{-1}, suggesting that such objects are triggered by low-intermediate luminosity AGNs hosted in their cores.

Considering the class of QSOs and ETS as a unique one, the sample results largely dominated by galaxies with an active nucleus (more than 70%). It is also worth noticing that the quasar population found in this sample is characterized by radio powers which are lower ($P= 10^{25\text{-}26}$ WHz^{-1}) than usually found for classical radio-loud QSOs. On the other hand, late type galaxies (LTS) have typically lower radio powers (3/5 have $P<10^{22}$ WHz^{-1}), as expected for radio sources triggered by star formation, and are found at lower redshifts ($z < 1$).

References

- Bolzonella M., Miralles J.M., Pellò R., 2000, A&A 363, 476B
- Donnelly R.H., Partridge R.B., Windhorst R.A., 1987, ApJ 321, 94
- Fomalont E.B., Windhorst R.A., Kristian J.A. et al., 1991, AJ 102, 1258
- Girardi L., Groenewegen M., Hatziminaoglou E. et al., 2005, A&A 436, 895
- Mignano A., Miralles J.M., da Costa L. et al., 2006, A&A in press
- Nonino M., Bertin E., da Costa L. et al., 1999, A&AS 137, 51
- Olsen L.F., Miralles J.M., da Costa L. et al., 2006, A&A in press
- Prandoni I., Gregorini L., Parma P. et al., 2000a, A&AS 146, 31P
- Prandoni I., Gregorini L., Parma P. et al., 2000b, A&AS 146, 41P
- Prandoni I., Parma P., Wieringa M.H. et al., 2006, A&A in press
- Windhorst R.A., Fomalont E.B., Partridge R.B. et al., 1993, ApJ 405, 498